$S=\frac{1}{2}$ chain in a staggered field: High-energy bound-spinon state and the effects of a discrete lattice

M. Kenzelmann,[1,2] C. D. Batista,[3] Y. Chen,[1] C. Broholm,[1,2] D. H. Reich,[1] S. Park,[2,4,5] and Y. Qiu[2,4]
[1]*Department of Physics and Astronomy, Johns Hopkins University, Baltimore, Maryland 21218, USA*
[2]*NIST Center for Neutron Research, National Institute of Standards and Technology, Gaithersburg, Maryland 20899, USA*
[3]*Center for Nonlinear Studies and Theoretical Division, Los Alamos National Laboratory, Los Alamos, New Mexico 87545, USA*
[4]*Department of Materials Science and Engineering, University of Maryland, College Park, Maryland 20742, USA*
[5]*HANARO Center, Korea Atomic Energy Research Institute, Daejeon, Korea*
(Received 23 September 2004; published 11 March 2005)

We report an experimental and theoretical study of the antiferromagnetic $S=\frac{1}{2}$ chain subject to uniform and staggered fields. Using inelastic neutron scattering, we observe a bound-spinon state at high energies in the linear chain compound $CuCl_2 \cdot 2((CD_3)_2SO)$. The excitation is explained with a mean-field theory of interacting $S=\frac{1}{2}$ fermions and arises from the opening of a gap at the Fermi surface due to confining spinon interactions. The mean-field model also describes the wave-vector dependence of the bound-spinon states, particularly in regions where effects of the discrete lattice are important. We calculate the dynamic structure factor using exact diagonalization of finite length chains, obtaining excellent agreement with the experiments.

DOI: 10.1103/PhysRevB.71.094411 PACS number(s): 75.25.+z, 75.40.Gb, 75.10.Pq

I. INTRODUCTION

When quantum particles interact, they can team up to form new particles with fractional charge or spin as observed in two-dimensional electron gases or low-dimensional spin lattices. A particularly fruitful model system to study emerging new particles and their interactions has been the antiferromagnetic (AF) $S=\frac{1}{2}$ Heisenberg chain. It does not order even at $T=0$ K due to strong quantum fluctuations and its elementary excitations are spinons carrying fractional $S=\frac{1}{2}$, which interact only weakly and are unbound particles.[1] Spinons were observed in several materials, including $KCuF_3$,[2] $BaCu_2Si_2O_7$,[3] and copper pyrazine dinitrate.[4] Strong interactions between spinons can arise from the breaking of spin rotational symmetry as, for example, in the three-dimensional coupled chain antiferromagnet where the mean field associated with the long-range ordered ground state restricts spin fluctuations. This creates an attractive potential for the spinons and at low energies they condense into spin-wave excitations carrying $S=1$,[5] as observed in $KCuF_3$ (Ref. 6) and $BaCu_2Si_2O_7$.[7]

Recently excitations were observed in the $S=\frac{1}{2}$ chain antiferromagnet $CuCl_2 \cdot 2((CD_3)_2SO)$ (CDC) subject to uniform and staggered magnetic fields which were interpreted as bound spinon states.[8] In the long-wavelength limit, the experiment demonstrated that the low-energy excitations of a $S=\frac{1}{2}$ chain in a staggered field correspond to the soliton and breather excitations of the quantum sine-Gordon model.[9] However, the sine-Gordon model is only valid for a very restricted range of wave vectors and does not apply for excitations at smaller length scales where the discreteness of the lattice becomes important. More importantly, it does not fully describe the mechanism by which the staggered field produces an attractive potential that binds spinons into the long-lived dispersive $S=1$ excitations as observed in the experiment.

In this paper, we analyze the dispersion of the observed bound-spinon states[8] in detail, and we report the observation of a bound-spinon state at high energies in CDC. In this system which has a nearest-neighbor exchange $J=1.5$ meV, a staggered field of the order of 1 T, which corresponds to a Zeeman energy $g\mu_B H \sim 0.1$ meV, qualitatively affects the excitation spectrum to energies more than twice J at 3.4 meV. This is in stark contrast to spinon binding in coupled chain magnets where the effects are only apparent for $\hbar\omega \approx k_B T_N$.[7] A simple mean-field theory of fermions carrying $S=\frac{1}{2}$ in one dimension captures the wave-vector dependence of the bound-spinon states, and explains the high-energy excitation through the opening of a gap at the Fermi surface. This model represents a first step towards a comprehensive description of the incommensurate excitations in AF $S=\frac{1}{2}$ chains subject to staggered fields.

II. EXPERIMENT

CDC was identified as an AF $S=\frac{1}{2}$ chain system in which a staggered g-tensor and/or Dzyaloshinskii-Moriya (DM) interactions[10,11] lead to a staggered field H_{st} upon application of a uniform field H. In CDC, a uniform magnetic field $\mathbf{H}=(0,0,H)$ along the c-axis generates a staggered field $\mathbf{H}_{st}=(H_{st},0,0)$ along the a-axis, and the Hamiltonian can be written as

$$\mathcal{H} = \sum_i J\,\mathbf{S}_i,\mathbf{S}_{i+1} - g_c\mu_B H S_i^z - g_a\mu_B H_{st}(-1)^i S_i^x, \qquad (1)$$

where g_c and g_a are the uniform part of the gyromagnetic tensor along the c and a-axis, respectively. The staggered field is given by

$$H_{st} = \frac{1}{2J}\frac{g_c}{g_a} DH + \frac{g_s}{g_a} H, \qquad (2)$$

where g_s is the staggered gyromagnetic form factor and $D=|\mathbf{D}|$ is the length of the DM vector, which points along the b-axis in CDC. The nearest-neighbor spin exchange

along the chain is accurately known from susceptibility measurements[11] and inelastic neutron scattering.[8] The spin chains run along the **a** axis of the orthorhombic crystal structure ($Pnma$),[12] with the Cu^{2+} ions separated by $0.5\mathbf{a}\pm 0.22\mathbf{c}$. Wave-vector transfer is indexed in the corresponding reciprocal lattice $\mathbf{Q}(hkl)=h\mathbf{a}^*+k\mathbf{b}^*+l\mathbf{c}^*$, and we define the wave-vector transfer along the chain as $q=\mathbf{Q}\cdot\mathbf{a}$. Due to weak interchain interactions, CDC has a long-range AF order in zero field below $T_N=0.93$ K with an AF wave vector $\mathbf{Q}_m=\mathbf{a}^*$. An applied field along the c axis suppresses the ordered phase in a second order phase transition at $H_c=3.9$ T,[10] indicating that interchain interactions favor correlations that are incompatible with the field-induced staggered magnetization.[13] At fields much greater than H_c, the staggered fields thus arise mostly from a staggered g tensor and DM interactions and not from interchain interactions.

The neutron scattering experiments were performed on 7.76 g of deuterated single-crystalline CDC. The measurements were carried out using the SPINS triple axis spectrometer and the DCS time of flight spectrometer at the NIST Center for Neutron Research. The SPINS measurements were performed with a focusing analyzer covering 7° in 2Θ scattering angle set to reflect $E_f=5$ meV to the center of the detector. A Be filter rejected neutrons with energies higher than 5 meV from the detection system. The measurements were performed with the strongly dispersive direction along the scattered neutron direction to integrate over wave vectors along weakly dispersive directions. The experimental configuration for the measurements made using the DCS spectrometer and the conversion of those data to absolute units are described in detail elsewhere.[8] They were performed with an incident energy $E_i=3.03$ meV and the incident beam parallel to the a axis for configuration A, and with an incident energy $E_i=4.64$ meV and angle of 60° between the incident beam and the a axis for configuration B.

III. EXPERIMENTAL RESULTS

Figure 1 demonstrates the dramatic changes that CDC undergoes upon application of a magnetic field. In zero field, the neutron scattering spectrum for $q=0.4\pi$ consists of a strong peak which corresponds to the two-spinon continuum, whose band width, at this wave vector is narrow and barely distinguishable from the experimental resolution. In a $H=9.86\ \mathrm{T}\simeq\frac{3}{4}J/(g\mu_B)$ field applied along the c axis, which also induces a staggered field along the a axis, the scattering includes two resolution-limited excitations. According to the quantum sine-Gordon theory, the lower-energy excitation corresponds to a bound-spinon state which develops into solitons and breathers at long wavelengths. The high-energy excitation at $3.4\ \mathrm{meV}\simeq 2.2J$, however, does not have a simple interpretation in terms of the sine-Gordon model. Its magnetic nature is apparent on account of its field dependence. The inset to Fig. 1 shows the dispersion of this excitation, which has a maximum at $q=0.4\pi$.

The dispersion of the high-field excitations at lower energies, $\hbar\omega<2$ meV, is illustrated in Fig. 2 for two different chain wave-vectors q. For $q=0.7\pi$, there are two maxima as a function of energy, corresponding to the well-defined

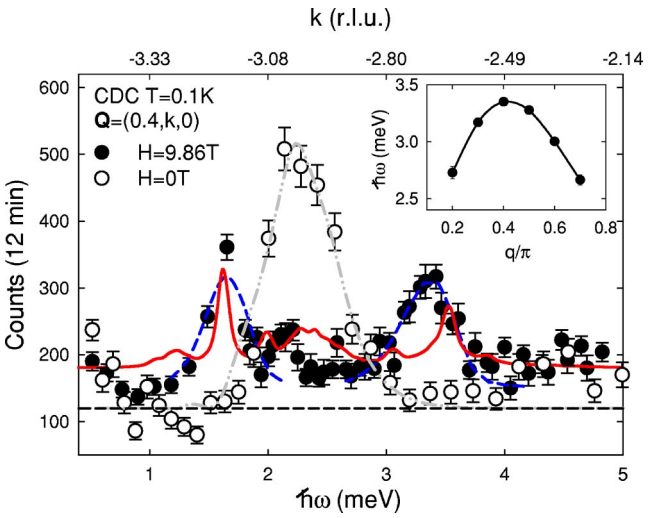

FIG. 1. (Color online) Neutron scattering intensity as a function of energy transfer for zero-field and 9.86 T measured using SPINS. The dashed line is a fit of two Gaussians convolved with the resolution function given by Cooper and Nathans (Ref. 14). The solid line shows the calculated intensity obtained from the exact diagonalization of finite chains for $H=11$ T and scaled to the data, with the nonmagnetic background given as the straight dashed line. The dashed-dotted line is the exact two-spinon cross section of the antiferromagnetic $S=1/2$ chain (Ref. 15) convolved with the experimental resolution function. Inset: Excitation energy of the higher-energy mode for $H=9.86$ T as a function of wave-vector transfer along the chain direction.

modes developing into the sine-Gordon soliton and breather excitations at long wavelengths. For $q=0.4\pi$, only one peak is clearly observed because of the weak intensity of one of the modes in this wave-vector region. The dispersion of these field-induced resonant modes was determined as a function of the chain wave vector, q, by fitting resolution-corrected Gaussian line shapes to the observed scattering. The adjusted excitation energies are shown in Fig. 3(a), illustrating that magnetic spectral weight generally shifts to lower energies in an applied field. However, due to the H_{st}-induced gap, this effect is much less pronounced than in a uniform field as the ground state energy increases.[16]

IV. MEAN-FIELD THEORY

We now present a simple mean-field theory of interacting $S=\frac{1}{2}$ fermions which captures both the emergence of a new excitation at high energies and the dispersion of the bound-spinon states. As it is well-known, a mean-field approach usually is not adequate to solve a one-dimensional system. This is because, for finite range interactions, the fluctuations are strong enough to preclude a nonzero value of an order parameter at any fine temperature. Moreover, if the order parameter is associated with a continuous symmetry, its mean value is zero even at $T=0$. Consequently, a mean-field theory that assumes a nonzero value of the order parameter with excitations that are originated by small fluctuations of such quantity cannot be a good description of a general one-dimensional system.

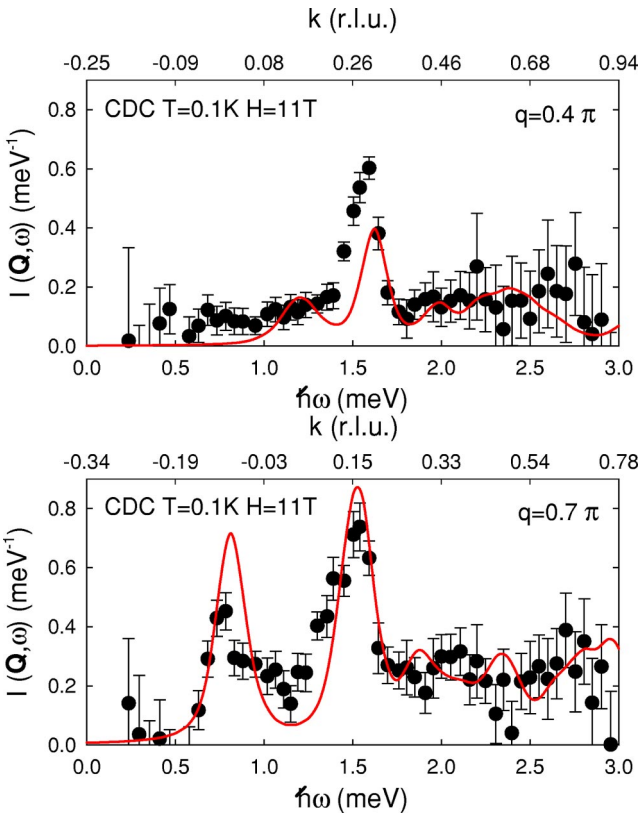

FIG. 2. (Color online) Neutron scattering intensity as a function of energy transfer at 11 T for two different chain wave vectors, measured using the DCS instrument with an incident energy E_i =4.64 meV. The solid line is the spectrum calculated from exact diagonalization of finite chains in absolute units, taking into account the polarization dependence of the experiment.

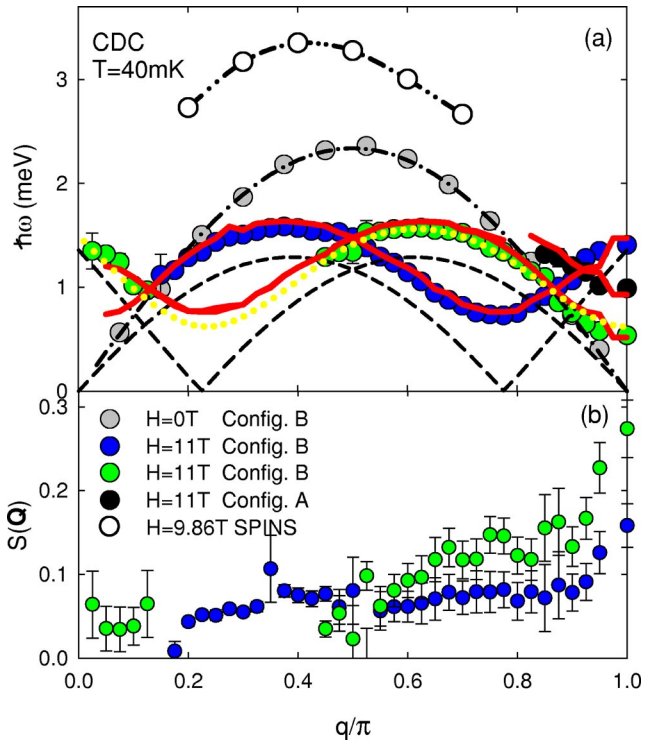

FIG. 3. (Color online) (a) Dispersion of the excitations at H =11 T and the lower bound of the zero-field two-spinon cross section (Ref. 17) obtained through fits to the zero-field data. The broken lines are predicted thresholds for continua for a $S=1/2$ chain in a uniform field (Ref. 16). The dashed-dotted line is the des-Cloizeaux-Pearson lower bound for excitations in $S=1/2$ chains in zero field (Ref. 18) for $J=1.5$ meV. The solid lines correspond to the dispersion obtained from Gaussian fits to the spectra obtained by the exact diagonalization of finite chains. The dotted line corresponds to the mean-field dispersion. The dashed double-dot line is a guide to the eye for the high-energy mode above 3 meV, which was measured at 9.86 T. (b) Integrated intensity of the two resonant modes at $H=11$ T as a function of wave-vector transfer.

In the present case, the system is invariant under rotations around the z axis for $H_{\rm st}=0$ and the candidate to be the order parameter is the xy planar component of the staggered magnetization $M_{\perp}^{\rm st}$. As expected for a continuous symmetry and a gapless spectrum, the system is critical at $T=0$, i.e., the order parameter has divergent fluctuations. However, the staggered field $H_{\rm st}=0$ couples linearly with the order parameter $M_x^{\rm st}$ along the x direction. Consequently, for $H_{\rm st}\neq 0$, the U(1) rotational symmetry is explicitly broken and the mean value of $M_x^{\rm st}$ becomes nonzero at any temperature. This also changes the nature of the excitations. The spinons (kink and antikinks) are no longer the low energy quasiparticles of the system since a pair of them is now confined by a linear potential. A similar effect occurs when we increase the dimension of the system due to the interchain interaction. Therefore we expect a mean-field treatment to be a good approach for high enough values of $H_{\rm st}$.

For $H_{\rm st}=0$, we know that the theory must be critical with the associated linear soft modes shown in Fig. 3(a). We also know that a one-dimensional spin system can be mapped into a fermionic system. In addition, a noninteracting fermionic Hamiltonian has a ground state that is also critical and has linear soft modes like the ones shown in Fig. 3(a). Therefore it is convenient to use a fermionic representation for the mean-field approach. For this purpose, the spin degrees of Cu^{2+} ions are described in terms of fermionic creation and annihilation operators:

$$S_j^{\nu}=\frac{1}{2}\sum_{\alpha,\alpha'} c_{j\alpha}^{\dagger}\sigma_{\alpha\alpha'}^{\nu}c_{j\alpha'}, \tag{3}$$

where $\nu=x,y,z$ and σ^{ν} are the Pauli matrices. Using this fermionic representation, Baskaran, Zou, and Anderson[19] proposed a mean-field theory (MFT) to treat low dimensional Heisenberg spin $S=1/2$ Hamiltonians. The MFT was generalized to SU(N) spin models (for large N) by Affleck and Marston.[20] Arovas and Auerbach[21] studied this theory in comparison with the Bethe Ansatz solution and showed that the fluctuation corrections are important in enforcing the Gutzwiller projection. Using an extended version of this MFT, we will study here the ground state properties and the spin dynamics of the $S=\frac{1}{2}$ chain in a staggered field given by $\mathcal{H}$.

Apart from an irrelevant constant, the expression for $\mathcal{H}$ in the fermionic representation is

$$\mathcal{H} = -\frac{J}{2}\sum_{i,\sigma,\sigma'} c^{\dagger}_{i\sigma}c_{i+1\sigma}c^{\dagger}_{i+1\sigma'}c_{i\sigma'} - \frac{g_c}{2}\mu_B H\sum_{i,\sigma}\sigma n_{i\sigma}$$

$$-\frac{g_a}{2}\mu_B H_{\rm st}\sum_{i,\sigma}(-1)^i c^{\dagger}_{i\sigma}c_{i\bar{\sigma}}, \quad (4)$$

with $\bar{\sigma}=-\sigma$. Since there is one spin per site, there is a constraint on the fermion occupation number: $n_i=\Sigma_\sigma n_{i\sigma}=1$ with $n_{i\sigma}=c^{\dagger}_{i\sigma}c_{i\sigma}$. For the Heisenberg term, we will use a linear combination of the mean-field decoupling introduced in Ref. 19 and the other natural decoupling in the presence of a staggered field along the x direction:

$$\mathcal{H}_{MF} = -\frac{J\gamma}{2}\sum_{i\sigma}(c^{\dagger}_{i\sigma}c_{i+1\sigma}+\text{H.c.}) - \frac{g_c}{2}\mu_B H\sum_{i,\sigma}\sigma n_{i\sigma}$$

$$-\frac{1}{2}(g_a\mu_B H_{\rm st}+J\delta)\sum_{i,\sigma}(-1)^i c^{\dagger}_{i\sigma}c_{i\bar{\sigma}}+\lambda\sum_i n_i, \quad (5)$$

where the Lagrange multiplier or chemical potential, λ, enforces the constraint of one spin per site at mean-field level. We are assuming translational invariance for γ_i, $\gamma_i=\Sigma_\sigma\langle c^{\dagger}_{i\sigma}c_{i+1\sigma}\rangle=\gamma$, and a staggered dependence for the effective field $\delta_i=\Sigma_\sigma\langle c^{\dagger}_{i\sigma}c_{i\bar{\sigma}}\rangle=\delta(-1)^i$. This staggered dependence is induced by the field $H_{\rm st}$. In momentum space, this leads to

$$\mathcal{H}_{MF} = \sum_{-\pi<k\leq\pi,\sigma}\Bigg[\left(-J\gamma\cos(k)-\frac{\sigma}{2}g_c\mu_B H\right)c^{\dagger}_{k\sigma}c_{k\sigma}$$

$$-\frac{1}{2}(g_a\mu_B H_{\rm st}+J\delta)(c^{\dagger}_{k+\pi\sigma}c_{k\bar{\sigma}}+c^{\dagger}_{k\bar{\sigma}}c_{k+\pi\sigma})\Bigg], \quad (6)$$

which can be written in the matrix formulation as

$$H_{MF}(k)_\sigma = \begin{bmatrix} -J\gamma\cos(k)-\sigma\frac{1}{2}g_c\mu_B H & -\frac{1}{2}(g_a\mu_B H_{\rm st}+J\delta) \\ -\frac{1}{2}(g_a\mu_B H_{\rm st}+J\delta) & J\gamma\cos(k)+\sigma\frac{1}{2}g_c\mu_B H \end{bmatrix}, \quad (7)$$

for $-\pi/2<k\leq\pi/2$. The eigenvalues of this matrix,

$$\epsilon^{\pm}_{k\sigma} = \pm\sqrt{\left(J\gamma\cos(k)+\sigma\frac{g_c}{2}\mu_B H\right)^2+\frac{1}{4}(g_a\mu_B H_{\rm st}+J\delta)^2}, \quad (8)$$

are the energies of the quasiparticle operators,

$$\alpha^{\dagger}_{k\sigma} = u_{k\sigma}c^{\dagger}_{k\sigma}+v_{k\sigma}c^{\dagger}_{k+\pi\bar{\sigma}},$$

$$\beta^{\dagger}_{k\sigma} = -v_{k\sigma}c^{\dagger}_{k\sigma}+u_{k\sigma}c^{\dagger}_{k+\pi\bar{\sigma}}, \quad (9)$$

with

$$u_{k\sigma} = \frac{\epsilon^{+}_{k\sigma}+J\gamma\cos(k)+\sigma\frac{1}{2}g_c\mu_B H}{\sqrt{\left(\epsilon^{+}_{k\sigma}+J\gamma\cos(k)+\sigma\frac{1}{2}g_c\mu_B H\right)^2+\frac{1}{4}(g_a\mu_B H_{\rm st}+J\delta)^2}}, \quad (10)$$

$$v_{k\sigma} = \frac{\frac{1}{2}g_a\mu_B H_{\rm st}+J\delta}{\sqrt{\left(\varepsilon^{+}_{k\sigma}+J\gamma\cos(k)+\sigma\frac{1}{2}g_c\mu_B H\right)^2+\frac{1}{4}(g_a\mu_B H_{\rm st}+J\delta)^2}}.$$

H_{MF} is diagonal in the new basis:

$$\mathcal{H}_{MF} = \sum_{-\pi/2<k\leq\pi/2,\sigma}(\epsilon^{+}_{k\sigma}\beta^{\dagger}_{k\sigma}\beta_{k\sigma}+\epsilon^{-}_{k\sigma}\alpha^{\dagger}_{k\sigma}\alpha_{k\sigma}). \quad (11)$$

The mean-field parameters γ and δ are given by the self-consistent equations:

$$\gamma = \frac{1}{2\pi}\sum_\sigma\int_{-\pi/2}^{\pi/2}\cos(k)(u^2_{k\sigma}-v^2_{k\sigma})[\langle\alpha^{\dagger}_{k\sigma}\alpha_{k\sigma}\rangle-\langle\beta^{\dagger}_{k\sigma}\beta_{k\sigma}\rangle]dk,$$

$$\delta = \frac{1}{2\pi}\sum_\sigma\int_{-\pi/2}^{\pi/2}u_{k\sigma}v_{k\sigma}[\langle\alpha^{\dagger}_{k\sigma}\alpha_{k\sigma}\rangle-\langle\beta^{\dagger}_{k\sigma}\beta_{k\sigma}\rangle]dk. \quad (12)$$

The value of λ is determined by imposing the average occupation per site to be equal to 1:

$$\frac{1}{2\pi}\sum_\sigma\int_{-\pi/2}^{\pi/2}[\langle\alpha^{\dagger}_{k\sigma}\alpha_{k\sigma}\rangle+\langle\beta^{\dagger}_{k\sigma}\beta_{k\sigma}\rangle]dk = 1. \quad (13)$$

When $H=H_{\rm st}=0$, the integration over the phase fluctuations of the local field γ_i (Ref. 21) renormalizes the value of γ given by Eq. (12): $\tilde{\gamma}=\pi\gamma/\sqrt{2}$. This renormalization improves considerably the comparison with the exact des-Cloizeaux-Pearson[18] two-spinon threshold ($\gamma_{ex}=\pi/2$). To improve the quantitative comparison of the MFT with the experiment and the exact diagonalization results, we will assume here that the same renormalization factor, $\frac{\pi}{\sqrt{2}}$, must be

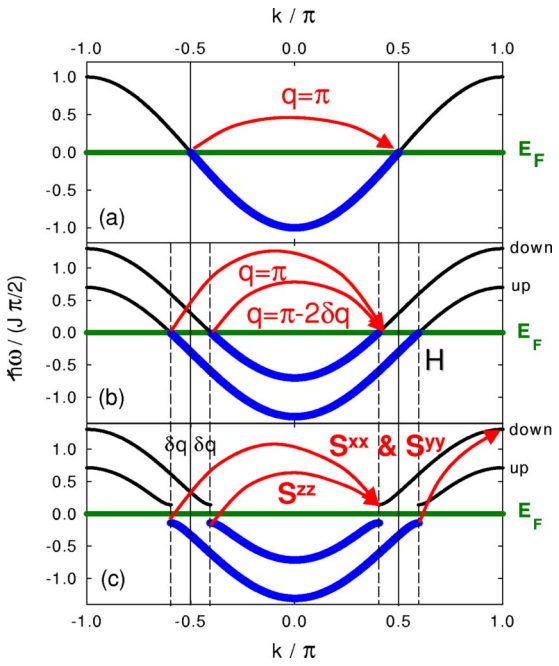

FIG. 4. (Color online) Schematic representation of the Fermi particle dispersion in (a) zero field, (b) uniform field H, and (c) uniform field H and staggered field H_{st} with $H>H_{st}$. In zero field the spin up and down particles with wave vector k have the same dispersion.

applied when H and H_{st} are finite. The value of γ is a measure of the effective strength of the spin fluctuations introduced by the Heisenberg term. More specifically, γJ is the Fermi velocity that in the original spin language corresponds to the velocity of the spinon excitations.

Figure 4 shows the evolution of the fermionic bands when the uniform and the staggered fields are applied. In the absence of these magnetic fields [Fig. 4(a)], there is only one band and the two-spinon cross section is associated with the continuum of particle-hole excitations. The dispersion relation for the lower branch is $\tilde{\gamma}J|\sin(q)|$. When a uniform magnetic field $H\neq 0$ is applied [Fig. 4(b)], the spin up and down bands are split by the Zeeman term. As a consequence, there is a change δq of Fermi wave vectors $|q_F|=\pi/2\pm\delta q$ and a corresponding change in the wave vectors of the zero energy modes: the energy of the transverse modes goes to zero at $q=\pi$ and $q=2\delta q$, while the longitudinal excitations have gapless modes at $q=0$ and $q=\pi-2\delta q$. From Eq. (8), the main effect of a nonzero staggered field H_{st} is to open a gap at the Fermi level, i.e., the fermionic system becomes an insulator and the spectrum is gaped for any excitation [Fig. 4(c)]. The gap results from the interband scattering which is introduced by the staggered field H_{st}. According to Eqs. (9), the degree of mixing is maximum at $q=q_F$. The emergence of this gap is consistent with the experimental data shown in Fig. 3(a).

To study the excitations of the new ground state induced by H_{st} it is necessary to calculate the neutron scattering cross section within our MFT. The neutron scattering cross section for the transverse excitations ($\nu=x,y$) at $T=0$ K is given by

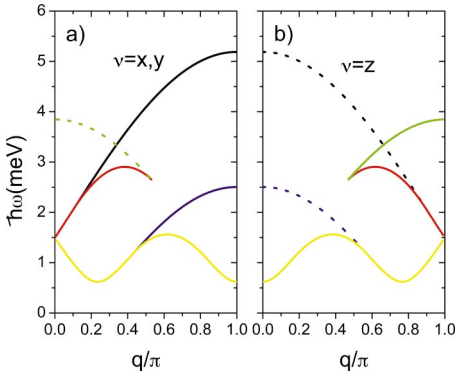

FIG. 5. (a) Transverse and (b) longitudinal excitations obtained from the mean-field theory, as described in the text in more detail.

$$S^{\nu\nu}(q,\omega)=\frac{1}{8\pi}\sum_{\sigma}\left[\int_{\pi/2-q}^{\pi/2}(u_{k+q\sigma}u_{k\sigma}+\eta v_{k+q\sigma}v_{k\sigma})^2\times\delta(\omega-\epsilon^{+}_{k+q\sigma}+\epsilon^{-}_{k\sigma})dk+\int_{-\pi/2}^{\pi/2-q}(u_{k+q\sigma}v_{k\bar{\sigma}}+\eta v_{k+q\sigma}u_{k\bar{\sigma}})^2\times\delta(\omega-\epsilon^{+}_{k+q\sigma}+\epsilon^{-}_{k\bar{\sigma}})\right]dk, \quad (14)$$

where $\eta=-1$ for $\nu=x$, $\eta=1$ for $\nu=y$, and $-\pi<q\leq\pi$. Note that in Eq. (14) $k+q$ must be contracted to the reduced Brillouin zone ($k+q\equiv k+q+n\pi$). The cross section for longitudinal excitations is

$$S^{zz}(q,\omega)=\frac{1}{8\pi}\sum_{\sigma}\left[\int_{\pi/2-q}^{\pi/2}(u_{k+q\bar{\sigma}}u_{k\sigma}+v_{k+q\bar{\sigma}}v_{k\sigma})^2\times\delta(\omega-\epsilon^{+}_{k+q\bar{\sigma}}+\epsilon^{-}_{k\sigma})+\int_{-\pi/2}^{\pi/2-q}(u_{k+q\sigma}v_{k\sigma}+v_{k+q\sigma}u_{k\sigma})^2\times\delta(\omega-\epsilon^{+}_{k+q\sigma}+\epsilon^{-}_{k\sigma})\right]dk. \quad (15)$$

Equations (14) and (15) reveal well-defined excitations that are determined by the cancellation of $d\omega/dk$, i.e., the divergence of the Jacobian. In Fig. 5(a) we show the different branches of the transverse excitations. The lower branch corresponds to the dispersion relation of the low energy excitations. In agreement with the experiment (see Fig. 3), there are two minima, one is located at the incommensurate wave vector $q_I=2\arcsin(g_c\mu_B H/2\gamma J)$ and the other one occurs at $q=\pi$. It is interesting to note that for $\nu=x$ the intensity of this branch goes to zero at $q_I=2\delta q$ due to a cancellation of the matrix element that multiplies the delta function in the integrand of Eq. (14). The black and the blue curves of Fig. 5(a) are the upper boundaries of interband particle-hole excitations associated with the transverse modes [Fig. 4(b)]. More specifically, the black curve results from excitations in which an electron is annihilated in the lower band and created in the upper band, while for the blue curve the process is the opposite. The green curve of Fig. 5(b) is the upper

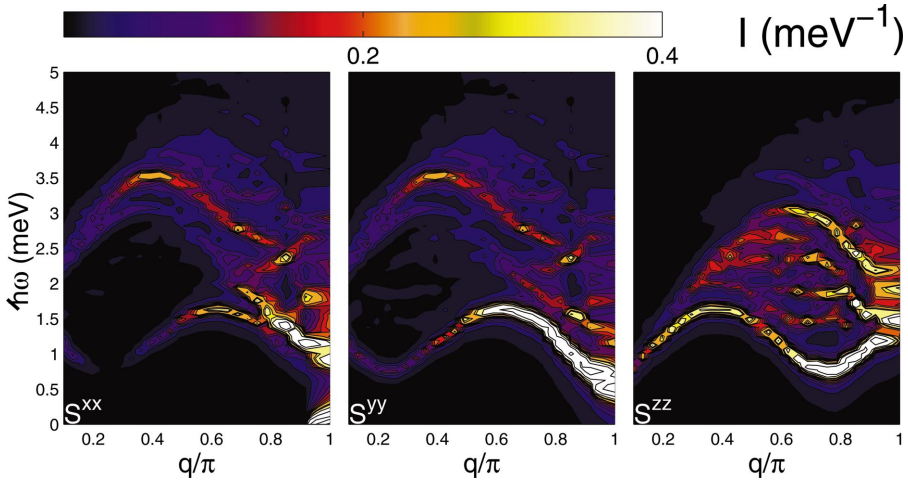

FIG. 6. The dynamic structure factors $S^{\alpha\alpha}(q,\omega)$ obtained through exact diagonalization of finite chains for $H_{st}=0.075H$, where $a=x$, y, and z are the spin polarizations. The uniform field is along the c axis (z polarization), the staggered field along the a axis (x polarization).

boundary for the intraband particle-hole excitations that describes the longitudinal modes. Note that these boundaries appear with dashed lines in the spectrum of excitations with the other polarization (Fig. 4). This is a consequence of the interband $q=\pi$ scattering which is introduced by the staggered field H_{st}. The dashed line just indicates that these "shadow" branches have a very small intensity.

The gap in the low energy spectrum is not the only qualitative change introduced by the staggered field H_{st} within the mean-field approach. Since the Fermi wave vectors $q_F=\pm\pi/2\pm\delta q$ are now extremal points of the new bands [see Fig. 4(c)], we expect the emergence of a new branch of transverse excitations associated with transitions between points that are close to $q_F=\mp\pi/2\pm\delta q$ ($q_F=\pm\pi/2\pm\delta q$) and points in the proximity of $q=0$ ($q=\pi$). This new branch of excitations [see the red curve in Fig. 5(a)] coincides with the new excitation which is experimentally observed at high energies (see Fig. 1), and thus explains our experimental results. For the longitudinal polarization, the new branch of excitations is shifted by π relative to the transverse polarization [see the red curve in Fig. 5(b)]. Since the maximum of this longitudinal branch is located at $q=\pi/2+\delta q$, it is difficult to distinguish this branch from the breathers in the experimental data. The energy of this maximum is close to 3 meV according to the MFT while the experimental value is 3.4 meV. This is reasonable given that the MFT is not an adequate approximation to give a quantitative description of the excitations.

V. EXACT DIAGONALIZATION OF FINITE LENGTH CHAINS

The intensities of the different branches are not properly described by the mean-field equations (14) and (15). For instance, the MFT predicts a high intensity for the upper boundary of the two-spinon excitations even at zero field for which very accurate calculations are available.[16] This is clearly an artifact of the MFT. To obtain an accurate description of the intensities and the energies of the different branches we complemented our analytical approach with the exact diagonalization of finite size chains. Using the Lanczos method, we obtained the exact ground state of H for finite chains of length $L=12,14,16,18,22,20$, and 24. Having the ground state, we computed the dynamical magnetic susceptibility, $\chi(\omega,q)$, for all the possible wave vectors $q=0, 2\pi/L, \ldots, 2\pi(L-1)/L$ of a chain of length L using the method introduced in Ref. 22. The wave vector $q=\pi$ is present in all of the considered chains. The small changes in the calculated $\chi(\omega,\pi)$ as a function of L indicate that the finite size effects are small for the considered problem. In general, smaller finite size effects are expected for systems that have an excitation gap because the spin-spin correlation length is finite.

The $T=0$ K structure factors were calculated using

$$S^{\alpha\alpha}(q,\omega)=\frac{1}{\pi}\chi''^{\alpha\alpha}(q,\omega). \tag{16}$$

The energy spectra were obtained by convoluting the discrete spectra for finite chains with Lorentzian functions with a full width at half maximum, $2\Gamma=0.1$ meV, in order to model the experimental energy resolution. The intensity of the calculated structure factors is given for a chain of L spins and normalized so that $\Sigma_{q,\alpha}\int d\omega S^{\alpha\alpha}(q,\omega)=S(S+1)$ as required by the total scattering sum rule.

The calculated neutron scattering for all chain lengths was averaged and the dynamic structure factor for the three different polarizations is shown in Fig. 6 as a function of wave-vector transfer and energy transfer for $H_{st}=0.075H$ on an absolute scale. The structure factor S^{zz} polarized along the uniform field contains a well-defined excitation with a minimum gap energy at an incommensurate wave vector. The structure factors S^{xx} and S^{yy} polarized perpendicular to the uniform field contain well-defined excitations whose dispersion has a minimum at the antiferromagnetic point, with S^{yy} having an excitation at a lower energy than S^{xx}. These excitations correspond to the first and second breather of the quantum sine-Gordon model.

Figure 6 also provides evidence that the excitation spectrum contains a substantial amount of continuum states, as observed in the experiment.[8] These states lie higher in energy than the well-defined low-energy excitations and extend to high energies. At $H_{st}=0.075H$ our numerical calculations

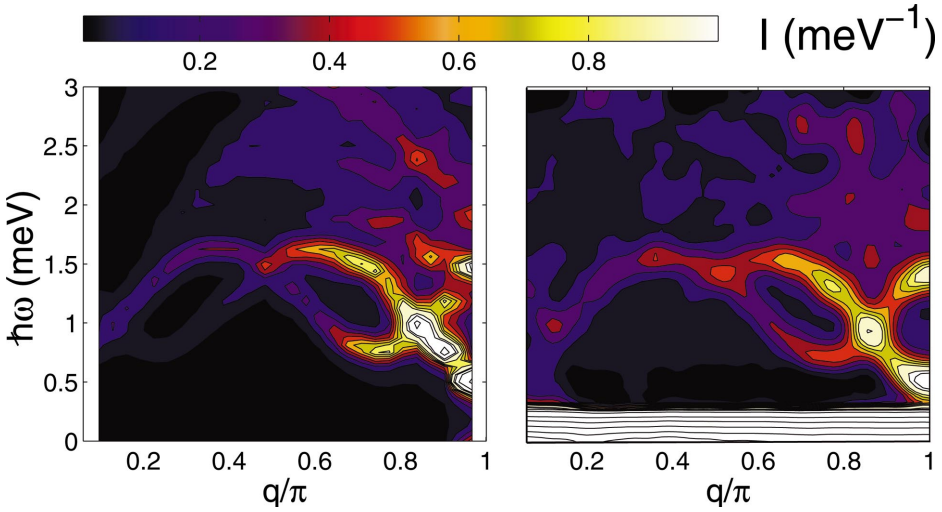

FIG. 7. (a) Calculated dynamic structure factor $S(q,\omega)$ for wave vectors and polarization of the DCS experiment. (b) Structure factor measured using DCS (Ref. 8).

yield an expectation value of the Hamiltonian per $S=\frac{1}{2}$ of $\mathcal{H}=-0.34J$, increased from the ground state energy at zero field, $\mathcal{H}=(\frac{1}{4}-\ln 2)J=-0.44J$, by $0.1J$.

The numerical data were binned and Gaussian fits were used to obtain excitation energies as a function of wave vector. These results are shown in Fig. 3(a) as a solid line, showing that the numerical calculations reproduce the dispersion relation of the low energy modes. We calculated the dynamic structure factor for the DCS experiment taking into account wave-vector dependent mixing of the polarized dynamic structure factor $S^{\alpha\alpha}$. Figure 7 directly compares the calculated and measured intensities on an absolute scale, showing that there is excellent agreement between the numerical calculations and the experiment.

In addition, Fig. 6 shows that a new branch of transverse magnetic excitations with the maximum around $q=0.4\pi$ and $\hbar\omega=3.5$ meV emerges when the staggered field is present. This provides a quantitative explanation for the high energy peak that appears in the neutron scattering data (see Fig. 1). Muller *et al.*[16] showed that this branch is not present for $H_{\mathrm{st}}=0$ by using macroscopic selection rules. For nonzero H_{st}, the total spin S and its projection along the z direction, S^z, are not good quantum numbers anymore, allowing the emergence of this new excitation. Our mean-field approach is in good agreement with this result.

VI. CONCLUSIONS

In summary, we have performed neutron scattering experiments, numerical calculations, and an analytical study investigating the AF $S=\frac{1}{2}$ chain in uniform and staggered fields. We found that the incommensurate bound-spinon states are well-described by a mapping to a interacting fermionic model after a renormalization of the energy. The model also explains the emergence of new excitations with the application of a staggered field. Our results suggest that the proposed mapping is more powerful than initial results suggested, and that it may also be useful for other quantum spin systems with a relatively short correlation length.

ACKNOWLEDGMENTS

Work at JHU was supported by the NSF through DMR-0306940. DCS and the high-field magnet at NIST were supported in part by the NSF through DMR-0086210 and DMR-9704257. C.B. and D.H.R. gratefully acknowledge discussions with A. J. Millis concerning the mean-field theory of $S=1/2$ chains.

[1] L. D. Faddeev and L. A. Takhtajan, Phys. Lett. A **85**, 375 (1981).
[2] D. A. Tennant, R. A. Cowley, S. E. Nagler, and A. M. Tsvelik, Phys. Rev. B **52**, 13368 (1995).
[3] M. Kenzelmann, A. Zheludev, S. Raymond, E. Ressouche, T. Masuda, P. Böni, K. Kakurai, I. Tsukada, K. Uchinokura, and R. Coldea, Phys. Rev. B **64**, 054422 (2001).
[4] M. B. Stone, D. H. Reich, C. Broholm, K. Lefmann, C. Rischel, C. P. Landee, and M. M. Turnbull, Phys. Rev. Lett. **91**, 037205 (2003).
[5] H. J. Schulz, Phys. Rev. Lett. **77**, 2790 (1996).
[6] D. A. Tennant, S. E. Nagler, D. Welz, G. Shirane, and K. Yamada, Phys. Rev. B **52**, 13381 (1995).
[7] A. Zheludev, M. Kenzelmann, S. Raymond, E. Ressouche, T. Masuda, K. Kakurai, S. Maslov, I. Tsukada, K. Uchinokura, and A. Wildes, Phys. Rev. Lett. **85**, 4799 (2000).
[8] M. Kenzelmann, Y. Chen, C. Broholm, D. H. Reich, and Y. Qiu, Phys. Rev. Lett. **93**, 017204 (2004).
[9] I. Affleck and M. Oshikawa, Phys. Rev. B **60**, 1038 (1999).
[10] Y. Chen *et al.*, (to be published).
[11] C. P. Landee, A. C. Lamas, R. E. Greeney, and K. G. Bücher, Phys. Rev. B **35**, 228 (1987).
[12] R. D. Willett and K. Chang, Inorg. Chim. Acta **4**, 447 (1970).
[13] M. Sato and M. Oshikawa, Phys. Rev. B **69**, 054406 (2004).
[14] M. J. Cooper and R. Nathans, Acta Crystallogr. **23**, 357 (1967).
[15] A. H. Bougourzi, M. Karbach, and G. Müller, Phys. Rev. B **57**, 11429 (1998).
[16] G. Müller, H. Thomas, H. Beck, and J. C. Bonner, Phys. Rev. B **24**, 1429 (1981).

[17] M. Karbach, G. Müller, A. H. Bougourzi, A. Fledderjohann, and K.-H. Mütter, Phys. Rev. B **55**, 12510 (1997).
[18] J. des Cloizeaux and J. J. Pearson, Phys. Rev. **128**, 2131 (1962).
[19] G. Baskaran, Z. Zou, and P. W. Anderson, Solid State Commun. **63**, 973 (1987).
[20] I. Affleck and J. B. Marston, Phys. Rev. B **37**, R3774 (1988).
[21] D. P. Arovas and A. Auerbach, Phys. Rev. B **38**, 316 (1988).
[22] E. R. Gagliano and C. A. Balseiro, Phys. Rev. Lett. **59**, 2999 (1987).